

CANDIDACY PROPOSAL
LOW MASS STAR FORMATION FROM PARSEC TO AU SCALES:
DEFINING THE PROPERTIES OF THE YOUNGEST PROTOSTARS
MELISSA ENOCH

1 Introduction

Much progress has been made in recent years toward an understanding of low mass star formation. Theoretical modeling, together with observations, provide a general picture of how an isolated low mass star forms, in which a rotating dense molecular core collapses to form a central protostar fed by accretion from a rotationally supported disk. Accretion is facilitated by a strong magnetic field, and excess angular momentum is carried away by a powerful bipolar outflow. When the protostar has accreted essentially all of its mass, it emerges as an optically visible pre-main sequence star with a disk and stellar wind. (Shu, Adams, & Lizano 1987). Empirically, this theoretical picture breaks down into four evolutionary stages: (1) A starless core phase before collapse commences; (2) A deeply embedded Class 0 phase with a central protostar surrounded by an infalling envelope, rapid accretion from a disk, and a powerful outflow. This stage is often defined by the envelope mass exceeding the protostellar mass, $M_{env} > M_*$; (3) A less embedded Class I phase with essentially the same structure as the Class 0 phase (protostar, disk, envelope, accretion, outflow), but where the protostar is now more massive than the envelope, $M_{env} < M_*$, and the outflow is less energetic; (4) An optically visible Class II phase consisting of a T Tauri star with a disk but no remaining envelope (André et al. 2000).

Most recent observations are largely consistent with this scenario, but many competing pictures describing the evolution in more detail exist. In particular, our understanding of how star formation in clustered regions differs from the isolated picture above is still developing. Fortunately, most viable models make observationally testable predictions. First, the mechanism of support for starless cores typically predicts the timescale for core evolution, or lifetime, τ . If thermal pressure is the only means of support, a core will begin to collapse when the mass exceeds the Jeans mass $M_J \propto \rho^{-0.5}$, and will have a lifetime comparable to the free-fall timescale ($\tau \sim t_{ff} \sim \text{few} \times 10^5 \text{yr}$). Models with magnetic fields as the main form of support predict that collapse will happen slowly through ambipolar diffusion; in this case the core lifetime is the ambipolar diffusion timescale ($\tau \sim t_{AD} \sim 10^7 \text{yr}$). Turbulent models predict lifetimes of a few dynamical timescales ($\tau \sim 8t_{dyn} \sim 10^6 \text{yr}$), as the turbulence decays via Alfvén waves (Ciolek & Mouschovias 1994; Li et al. 2000). Secondly, the initial structure of the core before collapse determines the mass accretion rate and radial density profile $\rho(r)$ of the protostar as it evolves, thereby providing a probe of the core initial conditions. For inside out collapse from a singular isothermal sphere (SIS), cores initially have a density profile $\rho \propto r^{-2}$. During collapse the infalling inner envelope is expected to have a $\rho \propto r^{-3/2}$ profile with a static r^{-2} outer envelope, and the accretion rate is constant, implying a Class 0 lifetime similar to the Class I lifetime (because the protostar accretes about half its mass in each phase). Alternatively, if collapse begins before relaxation to a SIS, cores would show a flattened inner density profile, with $\rho \propto r^{-1.7}$ in the outer regions. There will be a period of rapid mass accretion that decreases with time, thus Class 0 lifetimes are significantly shorter than Class I (Shu 1977; Foster & Chevalier 1993).

Two clear ways of differentiating between the above models are the radial density profiles ($\rho(r)$) and lifetimes (τ) of the starless core and Class 0 phases. If we make the assumption that star formation is homogeneous in space and time, an estimate of the statistical lifetime is given by the ratio of the number of sources in each class, e.g. $N_{class0}/N_{classI} = \tau_{class0}/\tau_{classI}$, where $\tau_{classI} = 2 \times 10^5 \text{yr}$ is relatively well determined by IR studies. It has been shown from starless

core lifetimes that some form of support beyond gas pressure is required (e.g. Ward-Thompson et al. 1994), and in a survey of isolated clouds Visser, Richer & Chandler (2002) find timescales inconsistent with ambipolar diffusion or a rapid mass accretion phase, but better statistics in a range of star forming environments are needed.

Other important observational tools that probe the initial conditions and very early phases of star formation include the clump mass function (MF) for clustered star formation, the protostellar binary frequency, and the velocity profile in the infalling envelope, $v(r)$, which is another measure of the accretion rate. A comparison of the prestellar clump MF to the stellar IMF may reveal the origin of the IMF shape. If stellar masses are determined by the protostars themselves through competitive accretion and feedback (e.g. outflows), we would not expect the emergent IMF to reflect the original clump IMF (Myer et al. 1999). If, on the other hand, stellar masses are determined by the initial fragmentation into cores, as might be expected in crowded regions where the mass reservoir is limited to a protostar's nascent core, the IMF should closely trace the clump MF. In Serpens (Testi & Sargent 1998) and ρ Oph (Motte et al. 1998) the clump MF appears to be similar to the stellar IMF, but more studies at the appropriate resolution are needed to establish if this result applies generally or depends on other factors such as environment. Measuring the frequency, separation and morphology of protostellar binaries helps to pinpoint when and how fragmentation into separate sources occurs. "Prompt initial fragmentation" from a loosely condensed cloud results in long period, separate envelope binaries, while fragmentation of an unstable accretion disk leads to a close, common disk binary. Interferometric arrays are necessary to resolve close binaries and separate envelope and disk emission. Looney et al. (2000) found a binary frequency of ~ 1 in embedded objects at high resolution, but the sample was small and biased toward very bright sources.

While there have been many previous studies undertaken to address the issues at hand, there is still much room for improvement, both in better statistics and more detailed high resolution studies. In a recent review, Evans (1999) identifies several areas of needed future research: A less biased census of early cores; improved measurements of envelope and core radial density profiles; interferometric observations to determine the early protostellar binary fraction; improved statistics on the clump MF; and high resolution spectroscopic observations to map kinematics close to the protostar. I plan to address aspects of each of these issues, with the goal of clarifying the star formation process from the collapse of prestellar clumps to energetic Class I protostars. I will examine star forming conditions and objects over a range of length scales, from cloud scales of ~ 10 parsecs to single core scales of $\sim 10^3$ AU, and evolutionary times, from starless cores to Class II objects, through a combination of the following projects:

- A large scale 1.1mm continuum map of the Perseus molecular cloud using Bolocam on the CSO. This map provides an unbiased, flux-limited sample of cores and protostars in a region of about six square degrees. Analysis will include mass and spatial distribution statistics, and ratios of the number of objects in different evolutionary stages to measure statistical lifetimes and accretion rates. Such measurements constrain core support mechanisms and infall models.
- Mosaiced observations of the B1 ridge, a hitherto unknown ridge of emission in Perseus identified in the Bolocam map, using the OVRO/CARMA interferometer at 3mm. Continuum data provide detailed radial density information for the starless cores within the ridge. A calculation of the clump mass function will be undertaken assuming a sufficient number of cores are found.
- The entire Perseus region will be covered by the Spitzer Legacy program, "From Molecular

Cloud Cores to Planet Forming Disks” (c2d; Evans et al. 2003), at wavelengths from $3.6\mu\text{m}$ to $70\mu\text{m}$. I will use data in the B1 ridge region to improve source statistics, source classification, and statistical lifetimes, as well as search for rare, faint or short-lived objects such as faint protostars within “starless” cores, or hydrostatic core formation.

- Follow-up $350\mu\text{m}$ SHARC2 and 3mm continuum OVRO/CARMA observations of selected sources in the Perseus cloud to allow detailed modeling of the radial density profiles and SEDs of starless cores and protostellar envelopes. Density profiles are diagnostic of collapse scenarios and initial conditions in pre-collapse cores.
- I am also carrying out a high resolution survey of known protostellar sources in the ρ Ophiuchi molecular cloud with OVRO, with continuing CARMA follow-up. High resolution interferometric continuum data at 3mm will facilitate the study of the detailed density structure and binary frequency of these sources. A large sample of protostellar binaries will place restrictions on the binary fragmentation mechanism. Simultaneous observations in HCO^+ and HCN molecular lines will map kinematics close to the protostars and hopefully separate the effects of collapse, outflow and rotation. A comparison of the ρ Oph results to those in Perseus will be important to test how protostellar and core properties vary with environment.

2 Protostellar cores in the Perseus Molecular cloud

Nearby molecular clouds such as Perseus, Ophiuchus, and Serpens, where there is considerable evidence of ongoing star formation (e.g. Evans 1999), provide the best opportunity to observe stars in the earliest stages of formation. Observationally, low mass star formation presents several distinct advantages. Low mass stars evolve less quickly than massive stars, are more numerous, not as highly obscured in their formation stages, and do not influence their environment as strongly, making it possible to extract clues about the initial conditions for formation. The earliest stages of star formation are, however, the most difficult to study observationally, with the embryonic star deeply embedded in an envelope of extinguishing gas and dust. Most of the observable continuum emission is re-radiated by the cool dust envelope, requiring observations at wavelengths longer than $\sim 10\mu\text{m}$. Submillimeter and millimeter observations are essential to trace core and envelope mass, and are probably the best way to directly observe starless cores, while IR observations are needed to detect the embedded protostars.

The Perseus cloud is often cited as an intermediate case between the low-mass, quiescent Taurus and turbulent, high-mass Orion star formation regions (e.g. Ladd et al. 1993). There have been a few molecular line observations of large portions of Perseus (e.g. the ^{13}CO map by Padoan et al. 1999; see Figure 1a), but most previous (sub)mm continuum and high resolution molecular line mapping has been confined to the dense cluster regions of NGC1333 and IC348. As part of the ancillary data set to the Spitzer c2d Legacy program, we observed approximately 7.5 square degrees of Perseus with Bolocam at the CSO (see Figure 1b). Bolocam is a 144 element bolometer array designed for mapping large fields at millimeter wavelengths, with a field of view of $8'$ and a beam of $30''$ at 1mm (Laurent et al. 2003). This map, observed in the $\lambda = 1.1\text{mm}$ mode during January/February 2003, represents the first unbiased, flux limited survey of cores and protostars in Perseus at millimeter wavelengths. With such a large sample over an extended region, it is possible to compare protostars in the wide range of star forming conditions present in Perseus. Within the cloud there are protostars and clumps in high density clusters (e.g. NGC1333) as well as in low density regions showing little dense molecular gas and no infrared emission (e.g. B1 ridge). A comparison of such regions will illuminate the conditions required for protostars to form. For

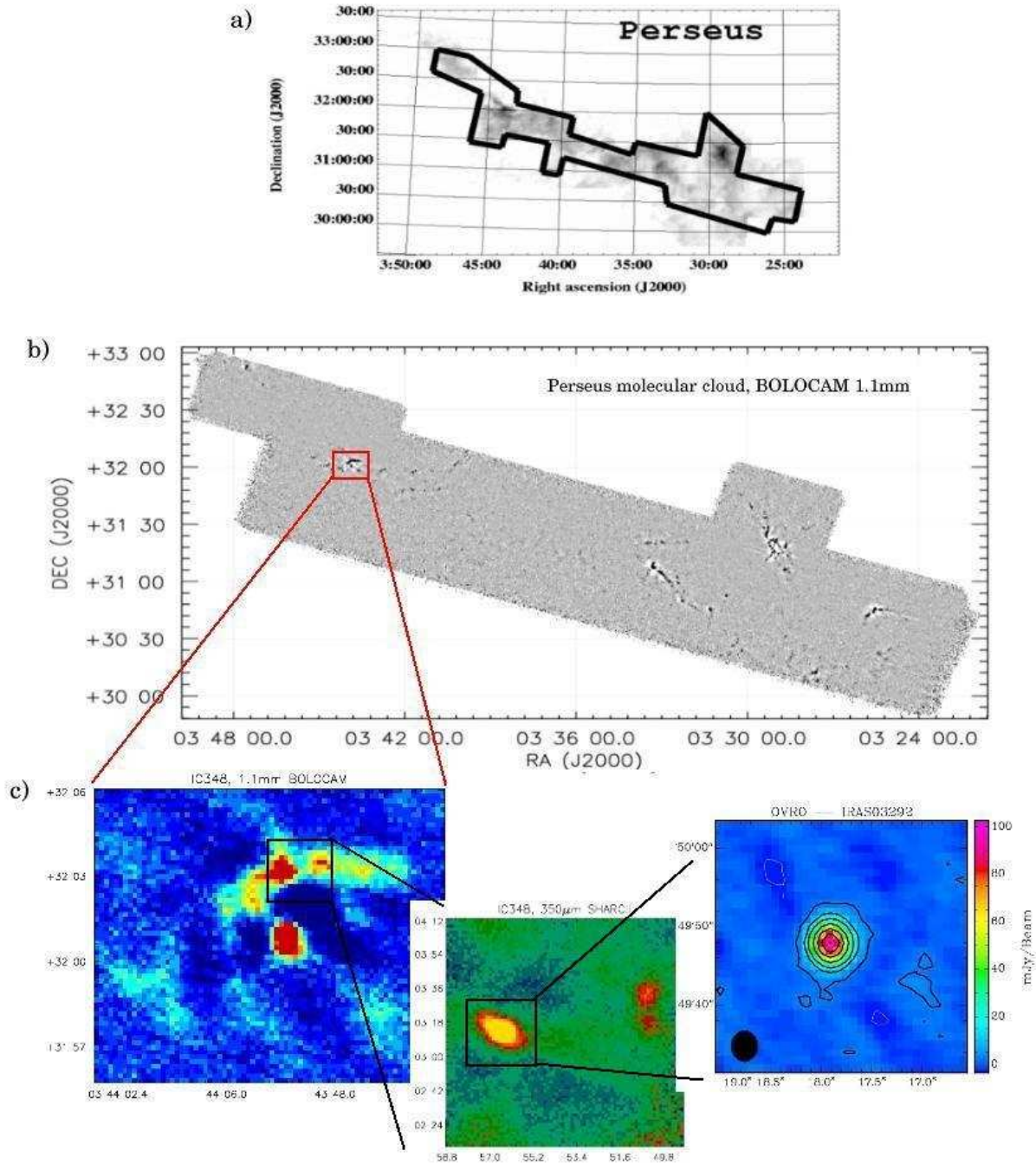


Figure 1: a) Planned Spitzer IRAC and MIPS observations (dark line; Evans et al. 2003) overlaid on a ^{13}CO map of Perseus from Padoan et al.(1999). The area covered to be is approximately the same as that observed with Bolocam. (b) The 1.1mm Bolocam map of Perseus; the large sample of objects will be exploited to improve statistics. Sources within the map are highly clustered, and large portions contain no 1mm flux. An analysis of the large scale structure present in this map, and how it compares to surveys such as the ^{13}CO map above, and the Spitzer observations of the same region, will be undertaken in order to understand how star formation proceeds within the cloud will form a fundamental part of this thesis. c) Example of follow-up observations with SHARC2 and OVRO. The region shown is near IC348 and contains several newly discovered protostars that will be mapped at high resolution ($\sim 5''$) with the OVRO interferometer. These follow-up observations will be used to study objects in varying density environments (SHARC2 and OVRO maps), and examine the structure of individual objects at high resolution (OVRO/CARMA).

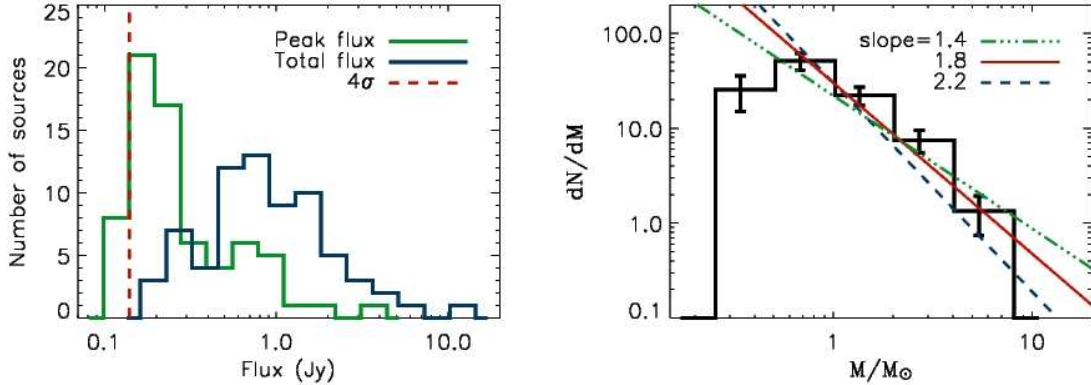


Figure 2: Some preliminary results from the Perseus survey – distribution of peak and total fluxes (left) and mass function (right) for all sources above 4σ in the BOLOCAM map. The best fit slope to the MF is $M^{-1.8}$.

example, finding a paucity of objects in low density regions as opposed to high density regions, would suggest that it is easier to form stars in pre-existing dense clumps.

Although much of the Bolocam data reduction software was in place at the time of observation, there is still much improvement to be made, including implementation of an iterative mapping routine to restore source flux removed by cleaning. I am continuing to work with the Bolocam instrument team to implement such a strategy, as well as on trouble-shooting reduction and mapping routines. After cleaning and mapping, a semi-automated routine for finding sources was applied, and positions, fluxes, sizes, and masses calculated. Assuming that the dust emission at 1mm is optically thin, the mass is computed as $M = D^2 S_\nu / \kappa_\nu B_\nu(T_D)$, where S_ν is the integrated flux, $\kappa_\nu \propto \nu^\beta$ is the dust opacity, and T_D is the dust temperature. I have completed some initial analysis of the data, with a few example results shown in Figure 2. The mean integrated flux of the sample is $\langle S_\nu \rangle = 1.3 \pm 1.6 \text{ Jy}$, the mean source size $\langle \text{FWHM} \rangle = 71 \pm 27''$, and the mean mass $\langle M \rangle = 1.6 \pm 1.3 M_\odot$. The 4σ detection limit is about 130mJy, or $0.15 M_\odot$ for a $T_D = 20\text{K}$ point source. The mass function, dN/dM as a function of M is also computed. The best fit slope to the MF is about 1.8, as shown in Figure 1b, however it must be noted that sources of all evolutionary classes are represented here, so the interpretation of this slope requires further analysis.

I am beginning a more careful analysis which will include an estimation of the dust temperature from a greybody fit to the SED, and a more thoughtful consideration of the dust opacity κ_ν . Sources with known IR fluxes will be classified according to the Class 0-II scheme. Classification methods include L_{bol}/L_{submm} , T_{bol} (the temperature of a blackbody with the same mean frequency), and M_{env}/L_{bol} . For successfully classified sources, an estimation of the statistical lifetimes will be made using the relative number of sources, as described in Section 1. I will also compute the mean separation of sources and undertake an analysis of their spatial distribution. The sources are highly clustered, with 48 of 70 having a companion within 3 arcmin (0.25pc), including essentially all of the bright sources. There are also large empty regions in the map with no apparent 1mm sources, raising the question of how star formation is proceeding through space in the cloud. The distribution of 1mm sources within the cloud is intriguing and will require further work, including a comparison to molecular and IR maps to examine, for example, how core formation correlates with A_V , dense gas tracers, and IR sources. Spitzer data will be very enlightening in this area, as it will find very faint protostellar sources down to $0.01 L_\odot$.

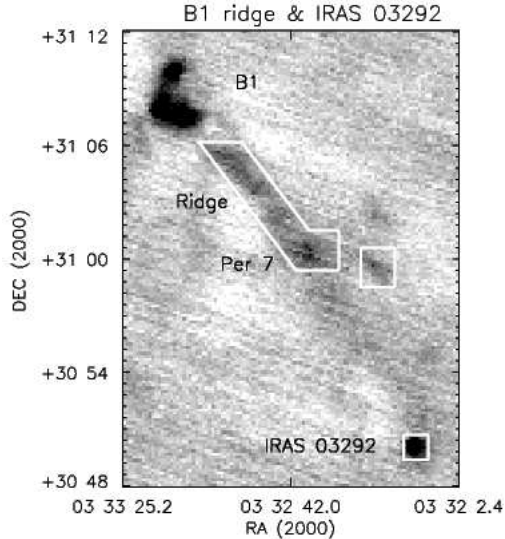


Figure 3: The B1 Ridge, and B1 (upper left) from the Bolocam map. This area contains many new sources found in the Bolocam map. I will be reducing and analyzing Spitzer data from this region, and comparing to the Bolocam data and continuing observations of the same area by SHARC2 and OVRO/CARMA. The white outlined regions are those covered by an OVRO mosaic observation (see Section 2.2) that will be used to calculate a clump mass function.

2.1 Clump mass function in the B1 Ridge

Based on our preliminary Bolocam results, a potentially interesting subsection of the Perseus cloud was targeted for a high resolution study with the OVRO interferometer (see Figure 3). The B1 ridge is a long ridge of extended 1mm emission below the bright cores of B1. The ridge is observed in gas tracers such as CO and CS (Bachiller et al. 1990), but contains no IRAS point source emission, suggesting the presence of a number of starless cores unresolved by the 30" Bolocam beam. The OVRO interferometer has approximately 10 times the resolution of Bolocam, and will easily resolve the sources in this extended ridge. A mosaic field of area $\sim 26 \text{ arcmin}^2$ was observed with 8 tracks at OVRO during Winter 2003/2004, with an effective beam size of 4". The full mosaic of 36 pointings has not yet been fully reduced, but if the number density and brightness of starless cores is similar to that seen in Serpens by Testi & Sargent (1998), the 26 arcmin^2 area covered should contain at least 28 cores, making a robust estimate of the clump MF down to $0.2M_{\odot}$ possible. Clump masses will be calculated in a similar way to that described for the Bolocam data. No measurements of the clump MF exist for Perseus, and such a study would test the universality of previous results found for other star forming regions.

2.2 Spitzer observations

As previously noted, the combination of IR and (sub)mm observations provides a powerful tool to study the very earliest phases of low mass star formation. Mid- and far-IR observations are difficult from the ground, but the Spitzer Space Telescope promises unprecedented sensitivity and resolution at wavelengths from $\lambda = 4 - 120 \mu\text{m}$. The c2d Spitzer Legacy project will map five nearby molecular clouds to find thousands of new protostars and cores, analyze their mass and space distributions, and determine the detailed form of the earliest stages of star formation. (Evans et al. 2003).

The c2d Legacy observations of the region shown in Figure 3 will form part of my dissertation research. Perseus is scheduled to be observed with IRAC and MIPS (3.6-70 μ m) in August 2004; the region to be observed overlaps almost entirely with the Bolocam map (see Figure 1a). As a c2d Associate I will be responsible for reducing and analyzing a portion of the data, specifically the region shown in Figure 3, for which SHARC2 and OVRO/CARMA follow up observations are currently ongoing. These observations will form part of my dissertation research. With these data it will be possible to classify all of the Bolocam sources by utilizing the new SED information, and the Bolocam sensitivity limit can be used to classify the numerous new sources that will be found by Spitzer. Hence, better evolutionary stage lifetimes will be estimated, placing stronger constraints on the validity of collapse models. Additionally, with a sensitivity limit of $\sim 0.01L_{\odot}$, the Spitzer data will ascertain whether some starless cores actually contain faint, early protostars, and the improved resolution over previous IR space telescopes will determine if each core contains one or many protostars. Finally, we hope the large sample available will allow us to see the very earliest, short-lived, stages of protostellar formation in which a hydrostatic core forms.

3 Modeling protostellar envelopes and prestellar cores

As already described, protostellar collapse models predict the radial density profile as a function of time, $n(r, t)$, for forming protostars. The initial conditions in the starless core phase ($\rho(r)$) are especially important, as they determine the early evolutionary history of the protostar (collapse dynamics, final mass, lifetime in each phase, etc). The observed $\rho(r)$ as a function of evolutionary class can be compared with theory as outlined in Section 1, but this requires a more careful analysis than many previous studies have undertaken, including a consideration of the variation of temperature with radius, real beam effects, and corrections to the Rayleigh-Jean approximation (Evans et al. 2001). We have observed several interesting Bolocam sources at higher resolution with both SHARC2 ($\lambda = 350\mu$ m, 9'' beam) and OVRO ($\lambda = 3$ mm, 4'' beam). The higher resolution observations are used to calculate the observed radial intensity profile $I(b)$, while the wide wavelength coverage constrains the SED, $S_{\nu}(\lambda)$.

I will model several protostellar envelopes and starless cores to determine the form of the density profile $\rho(r)$ using a modeling code developed by Shirley, Evans and others (e.g. Shirley et al. 2002). The modeling code takes into account heating from the central source and the interstellar radiation field, realistic beam effects, chopping, and variation of the dust opacity. A 1D radiative transfer code iteratively calculates the dust temperature as a function of radius, $T_D(r)$, using the density profile $\rho(r)$ and the observed SED as inputs. A single power law, inside out collapse, or pressure bounded Bonner-Ebert sphere may be used as the input $\rho(r)$. After convolution with the observational parameters, a model intensity profile $I_{\nu}(b)$ and SED $F_{\nu}(\lambda, \text{beam})$ are produced for comparison to the observed quantities.

Shirley et al. (2002) find that for Class 0 objects in their sample a single power law fits better than the inside out collapse model, while for starless cores a pressure bounded BE sphere is preferred over a SIS profile (Evans et al. 2001). More results are needed, however, as well as higher resolution to probe the inner profiles of cores. I have not yet begun a systematic application of the modeling code; initial tests using one of the brighter Bolocam sources indicates this source favors a power law density profile $\rho \propto r^{-p}$ with $p \sim 1.7$, and high central density. The model does not currently account for a disk component, which will increase the power law index, but the high resolution OVRO observations could break this degeneracy. Also, testing of theories with magnetic fields will have to wait for 2D models, as asymmetry must be included in those cases.

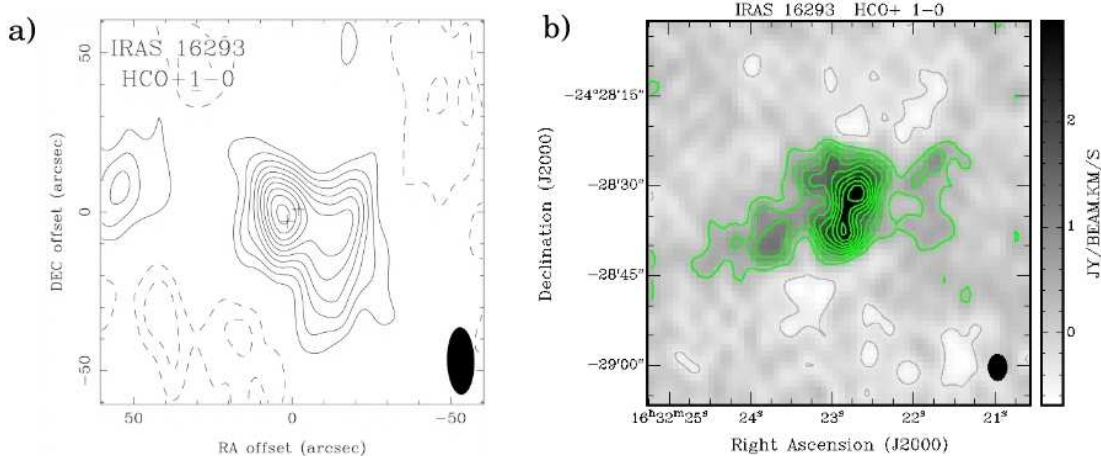


Figure 4: An example of expected results from the ρ Oph survey: velocity integrated HCO^+ emission in IRAS 16293. Left: Previous results from Choi et al. (1999) with a beam of $21'' \times 9''$. Right: OVRO results for this survey, with a beam of $5'' \times 4''$. The area covered is about 1/4 that in the Choi et al. map. Much more structure is evident, including a separation of IRAS 16293 sources A and B. We hope that high resolution observations in HCO^+ and HCN will begin to disentangle the effects of infall, outflow, and rotation in protostellar cores.

4 High resolution survey in Rho Ophiuchi

A large, targeted OVRO survey of starless cores and protostars in the ρ Oph cloud has recently been begun in collaboration with another student, Stuartt Corder. I will focus on the detailed envelope structure and kinematics as described below, while Stuartt will primarily use the sample to identify disk candidates for CARMA spectral line observations and subsequent modeling. The sample is chosen from the 1.3mm single dish surveys of André & Montmerle (1994) and Motte et al. (1998) on the basis of flux and compactness. With few exceptions these sources have not been previously observed at high resolution in the millimeter. We hope to image between 20 and 30 sources in 3mm continuum and HCO^+ and HCN lines, with a resolution of $5'' - 10''$.

My main goals for this project are: (1) Use high resolution maps to measure the binary frequency and the distribution of binary separations. Interferometric observations provide a unique tool for separating disk and envelope contributions, and for resolving embedded binaries. Binary frequency as a function of separation can point to different binary formation mechanisms (Looney et al. 2000), but current statistics for protostellar binaries are poor. (2) Utilize our improved resolution to constrain the radial density profile using the modeling method described in the previous section. High resolution measurements of $\rho(r)$ will strongly constrain core initial conditions and collapse models. The large sample available should greatly improve existing statistics. (3) Verify previous source classifications using morphology and SED information from the continuum maps, and outflow dynamics from HCO^+ ; use classifications to re-calculate statistical lifetimes. (4) Map outflows in HCO^+ and HCN at high resolution to trace outflow dynamics close to the protostellar sources. Ideally, we will acquire a large sample of outflows at different ages for comparison to other clouds and to theory. The mass, momentum and dynamical ages of outflows will also be calculated. (5) Identify infall candidates using HCO^+ and HCN line profiles as a function of position. Detecting collapse via blue-skewed profiles is complicated by both rotation and outflows, but interferometric observations maps help to disentangle these effects (Choi, Panis & Evans 1999). For starless

core infall candidates, apply for VLA observations to look for an accretion shock from a forming hydrostatic core.

A comparison of the statistical lifetime and radial density profile results for ρ Oph to those of Perseus will be important to test how such properties vary as a function of star forming environment. This project has only recently begun, and may ultimately raise questions in addition to those outlined above. CARMA follow-up observations will be necessary to accomplish many of these goals, and will clearly complement the current observations with higher resolution and observations in CO to map any interesting outflows. The VLA also presents opportunities for more detailed study of accretion shocks and outflow-driving jets at centimeter wavelengths.

5 Summary & Timeline

This thesis aims to attack outstanding issues in low mass star formation from several different fronts. The large surveys will improve statistics on source mass, size, and spatial distributions. Complementary high resolution studies help to understand in detail the structure and evolution of individual star forming objects at a range of evolutionary times. Observations will be obtained with a variety of telescopes and instruments, including single dish-bolometer arrays, interferometric radio arrays, and IR cameras.

- Spring/Summer 2004: Work with BOLOCAM team to refine reduction and analysis of Perseus 1mm data. Write Perseus Bolocam data paper. Reduce OVRO data for Perseus fields, including large mosaic in B1 Ridge; begin modeling of select Perseus sources.
- Fall/Winter 2004: Acquire, reduce & analyze Spitzer data for portions of the Perseus cloud. Compare Spitzer data with BOLOCAM, SHARC2 and OVRO data. Reduce OVRO data for ρ Oph targets.
- Spring 2005: Write analysis paper for Perseus sources. Begin analysis of continuum maps and spectral lines for rho Oph sources. Follow-up observations of individual Perseus and ρ Oph sources with CARMA. Apply for VLA follow-up if needed.
- Summer/Fall 2005: Write ρ Oph paper. Write B1 Ridge clump mass function paper. Continue follow-up CARMA observations in Perseus and ρ Oph as required.
- Fall/Winter 2005: Analyze follow-up data. Finish up papers. Apply for jobs.
- Spring/Summer 2006: Write & defend thesis.

6 References

- André, P. & Montmerle, T. 1994, ApJ, 420, 837
André, P. et al. 2000, in Protostars & Planets IV
Bachiller, K. M. et al. 1990, A&A, 236, 461
Choi, M., Panis, J-F., & Evans, N. J. II 1999, ApJS, 122, 519
Ciolek, G. E. & Mouschovias, T. C. 1994, ApJ, 425, 142
Evans N. J., II 1999, ARAA, 37, 311
Evans N. J., II et al. 2001, ApJ, 557, 193
Evans, N. J., II et al. 2003, PASP, 115, 965
Foster, P. N. & Chevalier, R. A. 1993, ApJ, 416, 303
Ladd, E. F. et al. 1993, ApJL, 410, 168
Laurent, G. et al. 2003, AAS Poster

Li, P. S. et al. 2000, BAAS, 32, 1393
Looney, L. W., Mundy, L. G., & Welch, W. J. 2000, ApJ, 529, 477
Motte, F., Andre, P., & Neri, R. 1998, A&A, 336, 150
Myers et al. 1999
Padoan, P., Bally, J., Billawala, Y., Jubela, M. & Nordlund, A. 1999, ApJ, 525, 318
Shirley, Y. L., Evans, N. J. II, Rawlings, J. M. C., & Gregersen, E. M. 2000, ApJS, 131, 249
Shu, F. H. 1977, ApJ, 214, 488
Shu, F. H., Adams, C. A. & Lizano, S. 1987, ARAA, 25, 23
Testi, L. & Sargent, A. I. 1998, ApJL, 508, L91
Visser, A. E., Richer, J. S. & Chandler, C. J. 2002, AJ, 124, 2756
Ward-Thompson, D. et al. 1994, MNRAS, 268, 276